Journal of Peptide Science
*J. Peptide Sci.* **10**: 291–297 (2004)
Published online 10 November 2003 in Wiley InterScience (www.interscience.wiley.com). DOI: 10.1002/psc.520

JOURNAL OF PEPTIDE SCIENCE

# Organization of Designed Nanofibrils Assembled from α-Helical Peptides as Determined by Electron Microscopy

**ANDREY V. KAJAVA,[a]*,‡ SERGEY A. POTEKHIN,[b] GIAMPIETRO CORRADIN[c] and RICHARD D. LEAPMAN[d]**

[a] Center for Molecular Modeling, CIT, National Institutes of Health, Bethesda, MD 20892, USA
[b] Institute of Protein Research, Russian Academy of Science, 142292 Pushchino, Moscow Region, Russia
[c] Institute of Biochemistry, University of Lausanne, Ch.des Boveresses 155, CH-1066 Epalinges, Switzerland
[d] Division of Bioengineering and Physical Science, ORS, National Institutes of Health, Bethesda, MD 20892, USA

*Received 23 April 2003*
*Accepted 16 June 2003*

Abstract: Self-assembling peptides present attractive platforms for engineering materials with controlled nanostructures. Recently, an α-helical fibril forming peptide (αFFP) was designed that self-assembles into nanofibrils at acid pH. Circular dichroism spectroscopy, electron-microscopy and x-ray fibre diffraction data showed that the most likely structure of αFFP fibrils is a five-stranded coiled coil rope. In the present study, scanning transmission electron microscopy (STEM) was used to improve our understanding of the αFFP fibril structure. The measurements of fibril mass per length suggest that there are ten α-helices in transverse sections of the fibrils. Based on the known data, it is proposed that a predominant fibrillar structure of αFFP is a dimer of α-helical five-stranded protofilaments wrapped around a common axis. It is shown that these structures have an axial dimension of $58 \pm 16$ nm and a width of $4 \pm 1$ nm. A small number of thin fibrils is also observed in the negative stained preparation and STEM images. The thin fibrils may correspond to the single protofilament. 

Keywords: α-helical coiled coil; design; fibrils; peptides; self-assembly

## INTRODUCTION

Molecular self-assembly as a tool for fabrication of defined nanostructures will have a significant impact in the coming decade. Numerous self-assembling systems have already been developed [1–3]. Polypeptides have not generally been considered to be useful for traditional materials science. Recent advances in genetic engineering and peptide synthesis have changed this view. Several spontaneously assembling peptides that form ribbons, tubes and fibrils have emerged as biological materials for diverse applications [4–6]. Most previously designed nanofibrils were made of peptides having β-structural conformations, while attempts to design α-helical nanofibrils led to fibrous aggregates that were unexpectedly large and exhibited an irregular thickness [7,8]. Recently, a 34-residue αFFP peptide was designed that is able to self-assemble into uniform soluble fibrils of diameter about 3 nm, which have their α-helices oriented along the fibril direction [9]. The unique fibril-forming ability of the designed αFFP opens new opportunities in biotechnology and medicine. For example, it was shown that covalent attachment of non-coiled coil peptides to αFFP does not disrupt the fibril formation. Such a fibrillar complex can be

*Correspondence to: Dr Andrey V. Kajava, CRBM, CNRS FRE-2593, 1919 Route de Mende, 34293 Montpellier, Cedex 5, France; e-mail: kajava@cnrs-mop.fr
‡ Present address: CRBM, CNRS FRE-2593, 1919 Route de Mende, 34293 Montpellier, Cedex 5, France.
Contract/grant sponsor: Swiss National Science Foundation; Contract/grant number: 7SUPJ048578.
Contract/grant sponsor: Russian Foundation for Basic Research; Contract/grant number: 98-04-50029.

used as a scaffold for construction of multivalent fusion proteins with attached biologically active ligands protruded from the fibril body. This property of $\alpha$FFP can provide a higher efficiency in a number of medical treatments and biotechnological processes [10,11]. Furthermore, being oriented these nanofibrils can form materials with anisotropic transmitting capabilities and can be applied in optics and nanotechnology. To improve the properties of $\alpha$FFP fibrils for particular applications it is important to know their atomic structure. However, the elongated shape and large molecular weight of the fibrils reduces the prospects for direct structural approaches such as x-ray crystallography or NMR to provide the necessary information. Molecular modelling showed that the diameter estimated by x-ray fibre diffraction analysis might fit the size of both four- and five-stranded $\alpha$-helical coiled coil ropes [9]. It is suggested that the five-stranded fibril is the most suitable model to explain the experimental data, but this model needs further experimental support. In this study, scanning transmission electron microscopy (STEM) was used to determine the mass per unit length of the fibrils [12,13]. These data provide additional constraints that further elucidate the structural arrangement of the peptides in the fibrils.

## MATERIALS AND METHOD

### Peptide Synthesis

Peptides were synthesized on a peptide synthesizer (Applied Biosystems 431A) and purified by RP-HPLC. The purity of peptides was analysed by RP-HPLC (C18 analytical column) and mass spectrometry. The peptide concentration was measured by the nitrogen determination method [14].

### Electron Microscopy

Thin films were evaporated from a carbon rod source onto freshly cleaved mica in an Edwards Auto 306 coating system (Edwards High Vacuum). The carbon films, approximately 3 nm in thickness, were floated off in de-ionized water and picked up on lacy Formvar/carbon films (EM Sciences) supported on 200 mesh copper grids. After the grids were blotted and dried, they were refluxed in acetone vapour to remove any residual hydrocarbons and were glow discharged in air immediately before use. The $\alpha$FFP peptide was dissolved in 100 mM sodium chloride maintained at a pH of 3.0 by the addition of HCl. For negative staining, a 5 µl aliquot of peptide solution at a concentration of about 0.1 µg/µl was applied to a grid and the peptide was allowed to adsorb for 2 min. The grid was then washed twice in de-ionized water before being negatively stained by adding a drop of 1% uranyl acetate. Excess fluid was blotted off and the grid was allowed to dry in air. Transmission electron micrographs were recorded using a CM120 electron microscope equipped with a GIF100 imaging filter imaging filter and a cooled slow scan CCD camera. Images were acquired and processed by means of the Digital Micrograph program (Gatan) running on a Power Macintosh 8500 computer. Image magnification was calibrated using a grating replica (EM Sciences).

STEM mass-per-length measurements were performed as described previously for other proteins [15,16]. A 5 µl aliquot of protein at a concentration of 0.1 µg/µl was first applied to a grid and was allowed to adsorb for 2 min. A 2 µl aliquot of tobacco mosaic virus at a concentration of 0.4 µg/µl was then injected into the drop and allowed to adsorb for 2 min, after which the specimen was washed by applying drops of deionized water and drawing off the excess liquid. The TMV was kindly supplied by Dr G. Stubbs of Vanderbilt University. The grids were partially blotted to maintain a thin layer of water and were immediately plunge-frozen into liquid ethane at $-180\,^{\circ}$C using a KF80 freezing device (Leica). Specimens were cryotransferred at $-170\,^{\circ}$C into a VG Microscopes HB501 STEM and were freeze dried by warming slowly to $-100\,^{\circ}$C [17]. After recooling the sample to $-170\,^{\circ}$C, annular dark-field images were acquired digitally at an accelerating voltage of 100 kV using a Gatan DigiScan system. The field emission source of the STEM provided a probe diameter of approximately 1 nm. Images containing $1024 \times 1024$ pixels were recorded with a 100 µs counting time per pixel to give an electron dose of approximately $10^3$ e/nm$^2$ and an acquisition time of 100 s. Images were transferred to an Apple Macintosh computer and were processed using the IMAGE program (National Institutes of Health). Integrated intensities in 20 nm lengths of the fibrils were measured and the average of two background intensities from adjacent regions of the support film were subtracted. Mass-per-length values were determined by measuring integrated intensities in similar lengths of TMV which has a known mass-per-length of 131 kDa/nm [12].

 

### Molecular Modelling

The structural model of a five-stranded protofilament with staggered $\alpha$-helices was modelled in our previous work [9]. The coiled coil structures, each containing 20 $\alpha$FFPs, were used to model a dimer of protofilaments. The initial arrangements of two five-stranded coiled coils that provide a maximal number of ionic and hydrogen bond interactions between the protofilaments were selected manually using INSIGHT II package [18]. The structure was refined further by the energy minimization procedure, based on the steepest descent algorithm (200 steps) implemented in the Discovery subroutine of INSIGHT II, and fixing backbone atoms. The final stage of minimization was 500 steps of the conjugate gradients algorithm. The distance-dependent dielectric constant was used for the energy calculations. Figure 5B and 5C were generated by the INSIGHT II package [18].

## RESULTS

### Number of $\alpha$FFP Molecules in the Fibril Cross-section as Determined by STEM

In negative stained preparations the $\alpha$FFP fibrils, formed at pH 3.0, appeared as uniform linear structures, which were sometimes bent or kinked (Figure 1A). The straight segments were typically 20–40 nm in length but the total fibrils length was as high as 60 nm. Although negative staining did not allow precise measurements of protein dimensions, it is estimated from the stain exclusion that the fibril width was in the range 3–5 nm. A few narrower structures were also visible with approximately half the width, i.e. 2 nm.

Low-dose scanning transmission electron microscopy (STEM) provided a quantitative measure of the fibril mass per unit length. Figure 1B is a STEM image of unstained $\alpha$FFP fibrils together with particles of tobacco mosaic virus, which was used as a mass calibration standard. After subtraction of background intensity due to scattering from the carbon film, the STEM intensity was directly proportional to the mass density. Eight STEM images similar to that in Figure 1B were analysed to obtain the mass per length distribution for a total of 192 $\alpha$FFP fibrils. The resulting data were plotted as a histogram in Figure 2, after binning in units of 1 kDa/nm. The histogram is well described by a single Gaussian peak centred at 7.95 kDa/nm, with

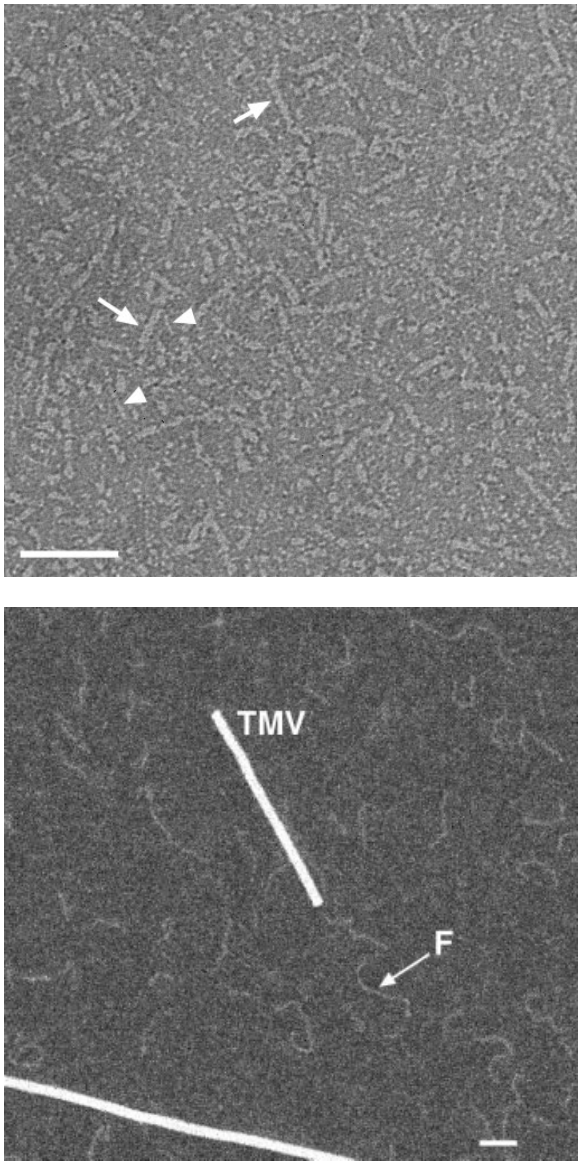


Figure 1 Electron micrographs of $\alpha$FFP assembled at pH 3.0: (A) TEM image of negative stained preparation; majority of fibrils have widths in range 3–5 nm (arrows) but some narrower structures of width approximately 2 nm are also observed (arrowheads). (B) STEM image of rapidly frozen and freeze dried preparation with tobacco mosaic virus used as a mass standard. Bars = 50 nm.

a standard deviation of 2.1 kDa/nm and a standard error of the mean of 0.15 kDa/nm ($n = 192$). There was also evidence for a much smaller population of narrower filamentous structures. This population was neglected in the mass per length measurements because of the low signal to background ratio and high statistical noise in the low dose STEM images.

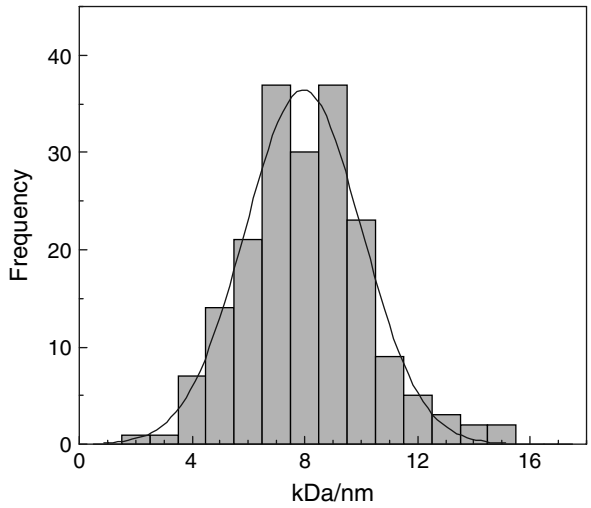


Figure 2 Histogram of fibril mass per length obtained from dark-field STEM measurements.

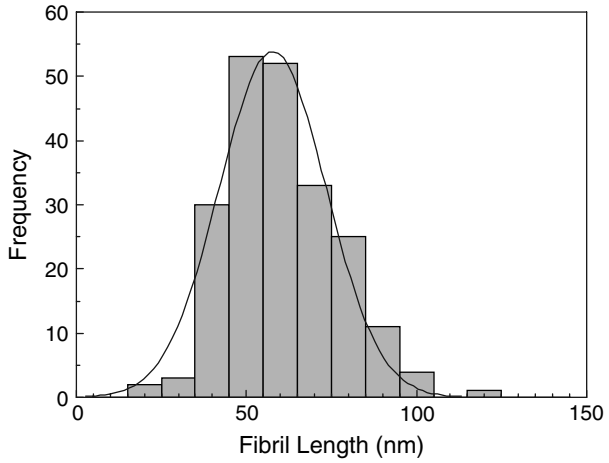


Figure 3 Histogram of fibril length distribution obtained from dark-field STEM measurements.

Circular dichroism spectroscopy of αFFP showed that its conformation within the fibrils was α-helical and x-ray fibre diffraction data suggested that these α-helices were oriented along the fibril axis [9]. These data together with the observed mass-per-length (MPL) value allowed the estimation of a number of peptide molecules in the cross-section of the fibrils. Indeed, for αFFP with a molecular mass of 4.085 kDa, the MPL of a single α-helix was 4.085 kDa/4.96 nm = 0.8235 kDa/nm. Therefore, our STEM data indicated that there were $(7.95 \pm 0.15)/0.8235 = 9.65 \pm 0.18$ (±sem) peptides in a cross section of the fibril, consistent with a stoichiometric value of 10 peptide molecules per cross section.

## Axial Dimensions of the Fibrils as Determined by STEM

Measurements of 214 fibrils in a total of eight STEM images like the one in Figure 1B gave a mean fibril length of 58 nm with a standard deviation of 16 nm (Figure 3). These fibrils appeared to contain straight segments as well as bends or kinks along their length. It was difficult to make accurate measurements of the fibril width from the STEM images due to possible lateral shrinkage of the structures after freeze drying but the widths appeared to be consistent with the estimated TEM values of 3–5 nm.

## Structural Interpretation of the STEM Data

The designed αFFP is a representative of α-helical coiled coil sequences that share a seven-residue repeat $(\mathbf{abcdefg})_n$ containing hydrophobic residues at positions **a** and **d** and polar residues generally elsewhere. Being folded in an α-helix this peptide had a hydrophobic side surface formed by leucine residues at **a**, **d** positions and also alanines at **e** positions. Polar or charged residues that occupied positions **b**, **c**, **f** and **g** form an opposite hydrophilic side of the α-helix. A transverse section through two possible arrangements of fibril is shown schematically in Figure 4, with each helix represented as a disk having hydrophobic (shadowed) and hydrophilic halves. Analyses of possible coiled coil structures show that the maximal number of strands for the coiled coil structures with the centre filled by hydrophobic side chains is five (Figure 4B) [19]. The six and more stranded coiled coil structures would have a central hole filled with water instead of the hydrophobic core (Figure 4A). For example, a ten-stranded coiled coil would have a central pore of about 2 nm. In this arrangement, the apolar side chains are exposed to the water and this makes coiled coil structures with more than five strands energetically unfavourable. This conclusion is in agreement with the experimental data. It is known that 20–50-residue long peptides with the α-helical coiled coil pattern form two-, three-, four-, and five-stranded bundles depending on slight variations in their sequences [20–22] while coiled coils with more than five strands are not observed.

 

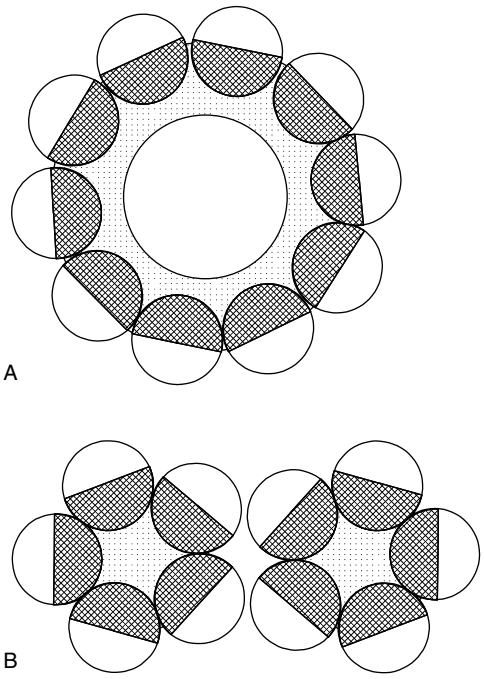


Figure 4 Schematic diagrams of two putative transverse sections of αFFP fibrils. (A) A ten-stranded α-helical fibril of about 5 nm diameter and 2 nm central pore. (B) Two five-stranded α-helical fibrils of diameter varying between 2.8 and 5.6 nm. Each circle represents a cross-section of an α-helix. Non-polar hydrophobic surfaces are shown by shadowed areas.

Knowing this, it is suggested that the ten-stranded αFFP fibrillar structures that were observed by STEM represent a dimer of five-stranded coiled coil structures, rather than a single ten-stranded coiled coil (Figures 4, 5). Indeed, molecular modelling showed that αFFP perfectly fit a five-stranded fibril with one-heptad axial shift of the adjacent α-helices [9]. The presence of the five-stranded coiled coil sub-structures is also in agreement with the data of x-ray fibre diffraction [9]. It was shown that the crystalline components of the αFFP specimen have a series of reflections that can be explained by a hexagonal packing of fibrils with a 2.5–2.8 nm distance between the adjacent fibrils. This is in the range of the known distances between five-stranded coiled coils observed in the crystals [20]. The dimeric fibrils with five-stranded protofilaments can be packed into such quasi-hexagonal array, while a crystal formed by a 5 nm wide ten-stranded coiled coil structure can not explain the observed x-ray pattern.

## DISCUSSION

The previously reported study showed that the diameter of the fibrils, α-helical conformation of the peptide and the orientation of α-helices along the fibril axis agree well with the five-stranded coiled coil arrangement [9]. In this work, the mass per length value of αFFP fibrils was determined using STEM. The results of these measurements suggest that the cross-section of the fibril has ten α-helices. It is speculated that the fibril consists of two five-stranded coiled coil protofilaments. It is worth mentioning, in this arrangement, that the interface of five-stranded coiled coils is formed by polar or charged side chains. Our molecular modelling shows that these side chains can form a network of hydrogen bonds between the glutamines at position **b**, **c** and ionic bonds between arginine and glutamine at positions **f** and **g** (Figure 5C). These patches of interactions are located regularly along the fibril axis and may control dimerization of the protofilaments. The coiling of the protofilaments around a common axis deforms their outside surfaces, which can make further lateral growth of the fibril impossible. Therefore the coiling can explain the limited diameter of the fibrils.

The strong tendency of protofilaments to dimerize explains why single five-stranded protofilaments are not abundant in the STEM images. Those single five-stranded protofilaments that are adsorbed to the support film may produce too small a signal to be visible in the noisy STEM images. This is consistent with previous measurements on negative stained preparations suggesting that there are thin and thick αFFP fibrils (Potekhin, personal communication). A small number of thin fibrils are indeed present in the negative stained preparation in Figure 1A.

The analysis of the fibril length distribution shows that the fibrils have a length limited to about $58 \pm 16$ nm (Figure 3). This result is in accordance with the previous sedimentation-diffusion study [9], which suggested that αFFPs assemble into elongated structures with a large-to-small radius ratio in excess of 20. The defined length of the fibrils may be important for their solubility, whereas most fibrils of unlimited length tend to precipitate into aggregates [7,8]. The interactions that control the length of the αFFP fibrils are not established yet. It might be, for example, due to the tension accumulated by the coiling of otherwise straight five-stranded protofilaments.

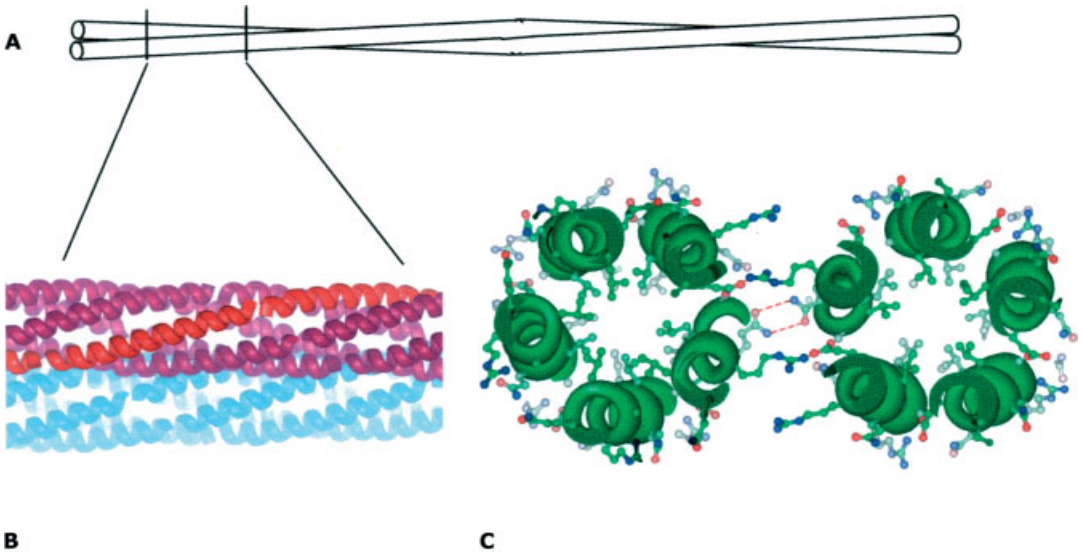


Figure 5 A structural model of the observed αFFP fibrils. (A) A general view of a fibril containing two protofilaments. (B) Enlarged picture of a region of the fibril shows two five-stranded α-helical ropes that correspond to each of the protofilament. α-Helices are shown by ribbons. Each strand is formed by the α-helices aligned head-to-tail. The five strands are wrapped around the coiled coil axis in a left-handed superhelix with parameters similar to the ones of the known pentameric coiled coil [20]. (C) An axial projection of the fibril demonstrates possible hydrogen bonds and ionic interactions between the protofilaments (shown by dotted lines). The backbone of the α-helix is present as a ribbon. Carbon atoms are in green, oxygen atoms are in red and nitrogen atoms are in blue.

In conclusion, this study demonstrates the presence of a fibrillar structure with ten α-helices in its transverse section. The number of α-helices is divisible by five, which is the number of α-helices in the coiled coil structure previously suggested by the x-ray fibre diffraction analysis [9]. In accordance with these data, it is proposed that two five-stranded coiled coil ropes tend to interact with each other and form thicker fibrils. The existence of the protofilamentous level of organization in the fibrils can be tested further by modifications of the αFFP sequence that may reduce or increase the ability of the protofilaments to associate. Depending on the modification, αFFP may form a single protofilament or a fibril containing more than two protofilaments, which may open additional opportunities for biotechnological applications.

## Acknowledgements

This work was funded in part by the Swiss National Science Foundation (grant 7SUPJ048578) and Russian Foundation for Basic Research (grant 98-04-50029).

## REFERENCES

1. Whitesides GM, Boncheva M. Beyond molecules: self-assembly of mesoscopic and macroscopic components. *Proc. Natl Acad. Sci USA* 2002; **99**: 4769–4774.
2. Lowe CR. Nanobiotechnology: the fabrication and applications of chemical and biological nanostructures. *Curr. Opin. Struct. Biol.* 2000; **10**: 428–434.
3. Reinhoudt DN, Crego-Calama M. Synthesis beyond the molecule. *Science* 2002; **295**: 2403–2407.
4. Marini DM, Hwang W, Lauffenburger DA, Zhang S, Kamm RD. Left-handed helical ribbon intermediates in the self-assembly of a b-sheet peptide. *Nano Lett.* 2002; **2**: 295–299.
5. Vauthey S, Santoso S, Gong H, Watson N, Zhang S. Molecular self-assembly of surfactant-like peptides to form nanotubes and nanovesicles. *Proc. Natl Acad. Sci. USA* 2002; **99**: 5355–5360.
6. Hartgerink JD, Beniash E, Stupp SI. Peptide-amphiphile nanofibers: a versatile scaffold for the preparation of self-assembling materials. *Proc. Natl Acad. Sci. USA* 2002; **99**: 5133–5138.
7. Pandya MJ, Spooner GM, Sunde M, Thorpe JR, Rodger A, Woolfson DN. Sticky-end assembly of a designed peptide fiber provides insight into protein fibrillogenesis. *Biochemistry* 2000; **39**: 8728–8734.

 

8. Ogihara NL, Ghirlanda G, Bryson JW, Gingery M, DeGrado WF, Eisenberg D. Design of three-dimensional domain-swapped dimers and fibrous oligomers. *Proc. Natl Acad. Sci. USA* 2001; **98**: 1404–1409.
9. Potekhin SA, Melnik TN, Popov V, Lanina NF, Vazina AA, Rigler P, Verdini AS, Corradin G, Kajava AV. *De novo* design of fibrils made of short alpha-helical coiled coil peptides. *Chem. Biol.* 2001; **8**: 1025–1032.
10. Pack P, Pluckthun A. Miniantibodies: use of amphipathic helices to produce functional, flexibly linked dimeric FV fragments with high avidity in *Escherichia coli*. *Biochemistry* 1992; **31**: 1579–1584.
11. Terskikh AV, Le Doussal JM, Crameri R, Fisch I, Mach JP, Kajava AV. 'Peptabody': a new type of high avidity binding protein. *Proc. Natl Acad. Sci. USA* 1997; **94**: 1663–1668.
12. Wall JS, Hainfeld JF. Mass mapping with the scanning transmission electron microscope. *Annu. Rev. Biophys. Biophys. Chem.* 1986; **15**: 355–376.
13. Engel A, Baumeister W, Saxton WO. Mass mapping of a protein complex with the scanning transmission electron microscope. *Proc. Natl Acad. Sci. USA* 1982; **79**: 4050–4054.
14. Jaenicke L. A rapid micromethod for the determination of nitrogen and phosphate in biological material. *Anal. Biochem* 1974; **61**: 623–627.
15. Leapman RD, Gallant PE, Reese TS, Andrews SB. Phosphorylation and subunit organization of axonal neurofilaments determined by scanning transmission electron microscopy. *Proc. Natl Acad. Sci. USA* 1997; **94**: 7820–7824.
16. Antzutkin ON, Leapman RD, Balbach JJ, Tycko R. Supramolecular structural constraints on Alzheimer's beta-amyloid fibrils from electron microscopy and solid-state nuclear magnetic resonance. *Biochemistry* 2002; **41**: 15 436–15 450.
17. Leapman RD, Andrews SB. Characterization of biological macromolecules by combined mass mapping and electron energy-loss spectroscopy. *J. Microsc.* 1992; **165**: 225–238.
18. Dayring HE, Tramonato A, Sprang SR, Fletterick RJ. Interactive program for visualization and modelling of proteins, nucleic acids and small molecules. *J. Mol. Graphics* 1986; **4**: 82–87.
19. Kajava AV. Modeling of a five-stranded coiled coil structure for the assembly domain of the cartilage oligomeric matrix protein. *Proteins* 1996; **24**: 218–226.
20. Malashkevich VN, Kammerer RA, Efimov VP, Schulthess T, Engel J. The crystal structure of a five-stranded coiled coil in COMP: a prototype ion channel? *Science* 1996; **274**: 761–765.
21. O'Shea EK, Klemm JD, Kim PS, Alber T. X-ray structure of the GCN4 leucine zipper, a two-stranded, parallel coiled coil. *Science* 1991; **254**: 539–544.
22. Harbury PB, Zhang T, Kim PS, Alber T. A switch between two-, three-, and four-stranded coiled coils in GCN4 leucine zipper mutants. *Science* 1993; **262**: 1401–1407.